

Electronic and magnetic structure of $\text{LaCuO}_{2.5}$

B. Normand and T. M. Rice

Theoretische Physik, Eidgenössische Technische Hochschule–Hönggerberg, CH-8093 Zürich, Switzerland

(Received 8 March 1996)

The recently discovered “ladder” compound $\text{LaCuO}_{2.5}$ has been found to admit hole doping without altering its structure of coupled copper oxide ladders. While susceptibility measurements on the parent compound suggest a spin gap and a spin-liquid state, NMR results indicate magnetic order at low temperatures. These seemingly contradictory results may be reconciled if in fact the magnetic state is near the crossover from spin liquid to antiferromagnet, and we investigate this possibility. From a tight-binding fit to the valence band structure computed in the local density approximation, we deduce that the strength of the interladder hopping term is approximately half that of intraladder hopping, showing that the material is three-dimensional in character. A mean-field treatment of the insulating magnetic state gives a spin-liquid phase whose spin gap decreases with increasing interladder coupling, vanishing (signaling a transition to the ordered phase) at a value somewhat below that obtained for $\text{LaCuO}_{2.5}$. The introduction of an on-site repulsion term, U , to the band scheme causes a transition to an antiferromagnetic insulator for rather small but finite values of U , reflecting the predominance of (one-dimensional) ladder behavior, and an absence of any special nesting features. [S0163-1829(96)03833-7]

I. INTRODUCTION

One of the interesting and challenging subfields of low-dimensional quantum magnetism which has emerged from the wealth of activity directed at improving the understanding of high-temperature superconductors is that of ladder systems.¹ These consist of n parallel, interacting chains of $S=\frac{1}{2}$ ions, which can be considered as a spin ladder with n legs, and rungs of $n-1$ bonds. The ladders have only weak mutual interactions. A combination of experimental and theoretical efforts has in the past few years produced significant advances in the realization and understanding of the properties of spin ladders, some of which are not at all intuitive.

Ladder cuprates emerged first with the discovery by Hiroi *et al.*² that in the series of materials $\text{Sr}_n\text{Cu}_{n+1}\text{O}_{2n+1}$ it is possible to create two-dimensional, stoichiometric copper oxide planes of composition $\text{Cu}_{n+1}\text{O}_{2n+1}$ by removing from the uniform CuO_2 plane parallel, equally-spaced lines of oxygen atoms. It was pointed out by Rice *et al.*³ that because these shear defects give rise to only weak, ferromagnetic interactions between neighboring copper spins, the remaining strips of CuO_2 plane will appear as isolated $(n+1)$ -leg ladders of antiferromagnetically coupled spins. These authors proposed that the systems should then illustrate the contrasting, and now well-established properties of even- and odd-leg ladders, that the former show a gap to spin excitations (spin gap) with consequent exponential spatial decay of correlations, while the latter are gapless with power-law decays. Subsequent susceptibility⁴ and nuclear magnetic resonance (NMR) (Ref. 5) experiments have amply borne out this conjecture.

The theoretical understanding of ladders has been in large part based on numerical techniques, which are particularly well suited to systems of such restricted dimensionality, and this is reviewed in Ref. 1. The first indications that the two-leg ladder should exhibit a spin gap came from numerical work,^{6,7} and a variety of methods has since been applied to

investigate the spin gap and spin correlations, and the properties of multileg ladders.^{8–10} These studies not only confirm the picture of the spin system emerging from analytic approaches¹¹ valid in certain limits, but provide the most accurate information available on the properties of this class of strongly-correlated systems.

The second proposal concerning the properties of ladder compounds made in Ref. 3, that the doped ladder should become superconducting with a d -wave order parameter, has proved harder to test for materials reasons. However, the compound $\text{LaCuO}_{2.5}$, recently synthesized by Hiroi and Takano,¹² has been found to admit hole doping without altering its structure of coupled, two-leg copper oxide ladders, and so constitutes the first case in which one may seek doping-dependent behavior analogous to that of the high-temperature superconductors. The high-pressure phase of $\text{La}_{1-x}\text{Sr}_x\text{CuO}_{2.5}$ is derived from a cubic, three-dimensional perovskite structure. The absence of oxygen atoms along lines leaves two-leg ladders which relax from a relative angle of 90° in the primitive structure to 62° in the depleted one. The material is then orthorhombic (space group $Pbam$), with four copper atoms per unit cell, and may be considered as a set of ladders oriented along the z axis, and periodically arrayed in the x and y directions, as shown in Fig. 1(a). This structure is not altered with Sr doping to $x=0.2$. The interladder coupling in the (x,y) plane arises because each oxygen atom at the outside edges of the two-leg ladders, which is part of the planar CuO_4 unit, is also effectively apical to a copper atom in a neighboring ladder, contributing to a finite transfer integral.

Susceptibility measurements¹² on the parent compound up to temperatures of 500 K, interpreted by a formula proposed by Troyer *et al.*,¹³ suggest the presence of a spin gap in the excitation spectrum, and therefore a spin liquid state. In contrast, NMR studies of the same samples¹⁴ indicate that the system orders antiferromagnetically at low temperatures, below an apparent $T_N \approx 117$ K. Since the spin susceptibility should evolve continuously as one passes through the quan-

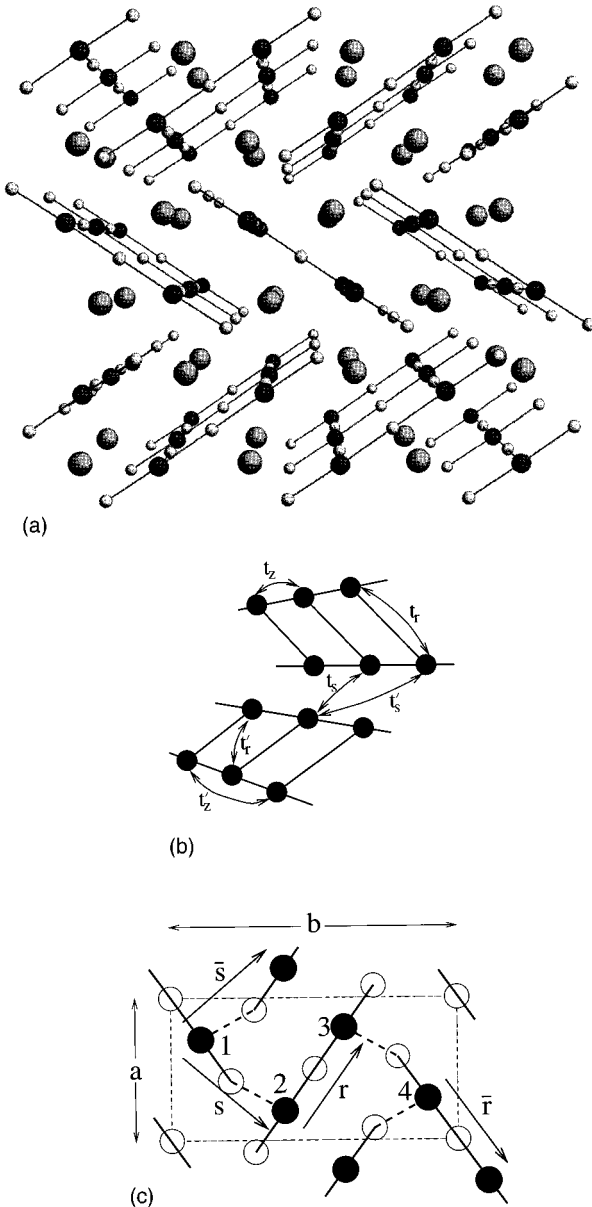


FIG. 1. (a) Crystal structure of the depleted perovskite $\text{LaCuO}_{2.5}$. Black and white spheres within the ladder units represent Cu and O atoms, respectively, and grey spheres represent Sr. The material is viewed along the axis of the ladders (\hat{z}), which can be seen to be rotated about this axis to a relative angle of 62° . In any (x, y) plane each copper atom is bonded to a neighbor in the same ladder by a rung bond, and to two copper atoms in neighboring ladders. The interladder couplings are through one oxygen atom which is bonded as part of the square planar coordination in the same ladder and is apical to a copper atom in the next ladder, and through the single apical oxygen atom, which is bonded in the ladder of the other neighbor. Allocation of antiferromagnetically arranged spins to each ladder shows that the material can exist as an unfrustrated antiferromagnet. (b) Schematic representation of $\text{LaCuO}_{2.5}$ to show the tight-binding parameters between Cu atoms used to fit the LDA band structure. (c) Appearance of the four inequivalent Cu atoms (black circles) in the unit cell. White circles represent O atoms. The vectors for the two types of bond in the (x, y) plane are $\mathbf{r}(\bar{\mathbf{r}}) = [0.5856a, -(+)0.2114b]$ and $\mathbf{s}(\bar{\mathbf{s}}) = [+(-)0.5a, 0.2886b]$, where $a \approx \sqrt{2}a_p$ and $b \approx 2\sqrt{2}a_p$ are the lattice constants in the x and y directions, and $a_p = c$ is the lattice constant of the original, cubic perovskite structure (Ref. 12).

tum critical point separating the spin-liquid state and the state with long-range antiferromagnetic order, it is possible that even in the latter, close to the quantum critical point, the spin susceptibility will decrease substantially as the temperature is lowered. Such behavior may be difficult to distinguish from that of a true spin liquid with a finite gap. Therefore it is plausible that the seemingly contradictory experimental results may be reconciled if the magnetic state is close to the crossover from an antiferromagnet to the spin liquid. Here we seek evidence, by examining the effects of interladder interactions, that the system is indeed close to this quantum critical point.

The outline of this paper is as follows. In Sec. II we present a tight-binding fit to the local density approximation (LDA) band structure to extract the interladder hopping matrix elements, and use these to obtain the superexchange interactions. We consider in Sec. III the nature of the spin-liquid ground state for ladders of spins coupled in both orthogonal directions, using a mean-field approach to estimate the location of the quantum critical point. In Sec. IV we introduce a double-occupancy term to the tight-binding bands, to investigate the degree of three-dimensional character in the electronic structure as a result of interladder interactions. Section V contains our conclusions and a brief discussion.

II. TIGHT-BINDING FIT TO THE LDA BAND STRUCTURE

The band structure of $\text{LaCuO}_{2.5}$ has been computed by Mattheiss,¹⁵ using the LDA method. Here we examine the dispersion of only the highest occupied valence bands, and use a tight-binding model based on the single, copper-based orbital in each planar CuO_4 unit within the ladder which lies closest to the chemical potential: in the $\text{Cu}_{n+1}\text{O}_{2n+1}$ strip this is the antibonding, Cu-centered $3d_{x^2-y^2}$ orbital. Restricting the set of hopping matrix elements to those between nearby copper atoms, we obtain an effective one-band model, albeit with four mixed levels (one from each Cu atom in the unit cell). These generate a complex of four bands, which lie close to or cut the Fermi energy. The complex is half-filled in the undoped system, and well separated from other bands on the small energy scales of most physical interest, so can be taken to determine the low-energy behavior of the model. With this interpretation, one may deduce the ratio t'/t , of inter- and intraladder atomic orbital overlap, and thus estimate the ratio J'/J of the magnetic interactions, by using the superexchange result¹⁶ $J \approx 4t^2/U$.

The tight-binding Hamiltonian is

$$H = - \sum_{ij\sigma} t_{ij} c_{i\sigma}^\dagger c_{j\sigma}, \quad (1)$$

in which i and j each denote a pair (n, m) , where n labels the unit cell, and $m = 1, \dots, 4$ the different atoms within each cell. The hopping matrix elements t_{ij} may be taken to be short ranged, and the maximal set which we need to achieve a reasonable fit is illustrated in Fig. 1(b). Starting from tight-binding parameter fits in the two-dimensional CuO_2 plane,^{17,18} we choose the nearest-neighbor intraladder parameters, t_r for hopping along a rung and t_z for hopping along a

leg, to have the same value $t_r = t_z = t \approx 0.4$ eV. We use as the next-nearest-neighbor parameters $t'_r = -\frac{1}{5}t_r$ and $t'_z = \frac{1}{6}t_z$ for hopping across a square plaquette in the ladder, and along two leg bonds, respectively. Finally, we introduce a parameter t_s for hopping from a copper atom on one ladder to its neighbor on the adjacent ladder, and also the next-neighbor analog t'_s for transfer between atoms on adjacent ladders with a relative displacement of one leg bond. Because of the low symmetry of the $\text{LaCuO}_{2.5}$ structure, the Cu-(apical) O-Cu interladder bond is far from straight, with the CuO_5 pyramids quite irregular, and this distortion may allow a substantial value of t_s . The role of each of the terms in the fitting scheme will be illustrated below. The next-neighbor parameters $t'_{r,s,z}$ are expected to be significantly smaller than their direct counterparts, due to the short-range nature of the overlaps, and the important parameter to fit will be the ratio of t_s to t_r .

The Hamiltonian (1) may be expressed in matrix form in reciprocal space as

$$H = \sum_{\mathbf{k}\sigma} \mathbf{c}_{\mathbf{k}\sigma}^\dagger \mathbf{H}_{\mathbf{k}} \mathbf{c}_{\mathbf{k}\sigma}, \quad (2)$$

where $\mathbf{c}_{\mathbf{k}\sigma}^\dagger = (c_{\mathbf{k}\sigma}^{1\dagger}, c_{\mathbf{k}\sigma}^{2\dagger}, c_{\mathbf{k}\sigma}^{3\dagger}, c_{\mathbf{k}\sigma}^{4\dagger})$ is the vector of creation operators

$$c_{\mathbf{k}\sigma}^{m\dagger} = \frac{1}{\sqrt{N}} \sum_n e^{i\mathbf{k}\cdot\mathbf{R}_{n,m}} c_{n,m\sigma}^\dagger \quad (3)$$

for the Bloch states formed by separate linear combination of the $d_{x^2-y^2}$ orbitals of each copper atom in the unit cell, and \mathbf{k} is a vector in the orthorhombic Brillouin zone. Setting the lattice constants a , b , and c to unity, the Hamiltonian matrix is

$$\mathbf{H}_{\mathbf{k}} = - \begin{pmatrix} t_z(k_z) & \bar{t}_s e^{ik_y s_y} & 0 & \bar{t}_r e^{-i\mathbf{k}\cdot\bar{\mathbf{r}}} \\ \bar{t}_s e^{-ik_y s_y} & t_z(k_z) & \bar{t}_r e^{i\mathbf{k}\cdot\mathbf{r}} & 0 \\ 0 & \bar{t}_r e^{-i\mathbf{k}\cdot\mathbf{r}} & t_z(k_z) & \bar{t}_s e^{ik_y s_y} \\ \bar{t}_r e^{i\mathbf{k}\cdot\bar{\mathbf{r}}} & 0 & \bar{t}_s e^{-ik_y s_y} & t_z(k_z) \end{pmatrix}, \quad (4)$$

where $t_z(k_z) = 2t_z \cos k_z + 2t'_z \cos 2k_z$, $\bar{t}_s = 2\bar{t}_s \cos \frac{1}{2}k_x$, in which the factor $\cos \frac{1}{2}k_x$ arises because $s_x = 0.5$, $\bar{t}_v = t_v + 2t'_v \cos k_z$, and the bond vectors $\mathbf{r}(\bar{\mathbf{r}})$ and $\mathbf{s}(\bar{\mathbf{s}})$ are shown in Fig. 1(c). The eigenvalue problem gives an equation quadratic in the squares of the mode frequencies, whose solutions are the dispersion relations of the four energy bands

$$\epsilon_{\mathbf{k}} = \pm [\bar{t}_r^2 + 4\bar{t}_s^2 \cos^2 \frac{1}{2}k_x \pm 4\bar{t}_r \bar{t}_s \cos \frac{1}{2}k_x \cos \frac{1}{2}k_y]^{1/2} - 2t_z \cos k_z - 2t'_z \cos 2k_z. \quad (5)$$

This concise, closed form emerges because the exponential factors $e^{\pm(2ik_y r_y + 2ik_y s_y)}$ may be collected as $1 - \cos k_y$, as $r_y + s_y = 0.5$. The general dispersion simplifies further for particular values of k_x and k_y in the Brillouin zone: in particular, on the zone faces ($k_x, k_y = \pi$), the last term in the square root vanishes and the bands are doubly degenerate, as required by the group-theoretical analysis of structures with nonsymmorphic space groups.

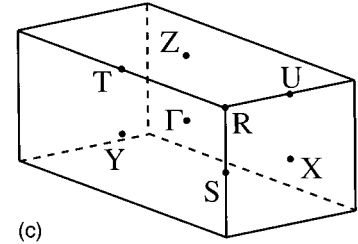
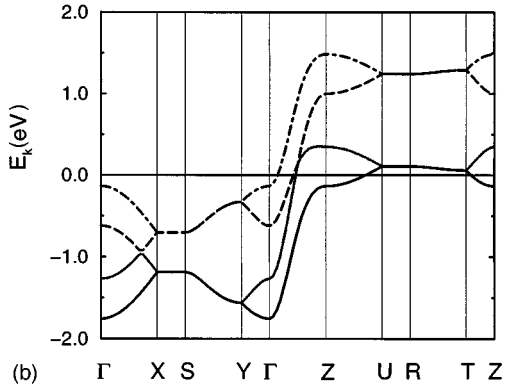
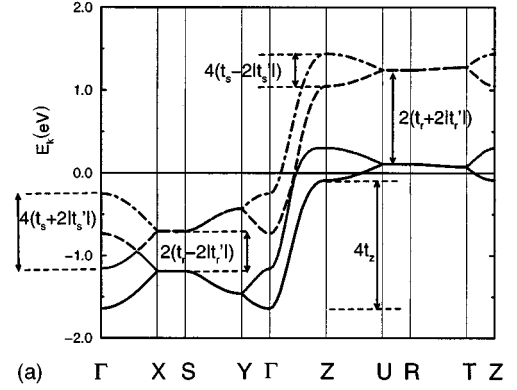


FIG. 2. (a) Illustration of the effects of the chosen band structure parameters on the observed dispersion curves, for the choices $t_z = t_r = t = 0.4$ eV, $t'_z = \frac{1}{6}t_z$, $t'_r = -\frac{1}{5}t_r$, $t_s = \frac{2}{3}t_r$, and $t'_s = \frac{1}{5}t_s$. (b) Tight-binding band structure for the parameter set which appears closest to the LDA results of Mattheiss (Ref. 15). Parameters are as in (a), but with $t_s = \frac{1}{2}t_r$. Details of the fitting procedure and parameter choices are given in the text. (c) Notation for \mathbf{k} points in the orthorhombic Brillouin zone.

The dispersions of the four bands are shown in Fig. 2(a) for a series of high-symmetry lines in the orthorhombic Brillouin zone, and for the ratio $t_s/t_r = 0.4$. The labeling of points is shown in Fig. 2(c), and their order is chosen to match the results of Mattheiss.¹⁵ Also shown in the figure are the energy spacings dictated by the choice of the tight-binding parameters, as these vary between their maximum and minimum values along the chosen directions.

For an isolated ladder along \hat{z} , i.e., with no interladder interactions ($\bar{t}_s = 0$), the bands would be completely flat around $\Gamma XSY\Gamma$ and $ZURTZ$, with only a cosine dispersion (mildly perturbed by the t'_z term) along ΓZ . In this situation there would be two doubly-degenerate bands around the zone center and zone face, corresponding to the bonding and

antibonding bands of each ladder. These features are reflected in the two branches observed in Fig. 2(a). From Eq. (5), the separation of the degenerate bands along the zone face XSY and edge URT is governed by the combinations $t_r \pm 2t'_r$ and the splitting of the degeneracy along ΓX , ΓY and ZU , ZT by the combinations $t_s \pm 2t'_s$. Considering first the intraladder parameters t_z , t'_z , t_r , and t'_r chosen from the two-dimensional CuO_2 plane, we find good agreement of the tight-binding result with that from LDA. Particularly notable is that the negative sign of t'_r and the relative magnitude $\frac{1}{5}t_r$, are required to reproduce the bands separations along XSY and URT . There is no evidence that a value of t_r different from t_z would improve the fit. The next-neighbor hopping parameter along the ladder, t'_z appears only as an asymmetry of the cosine dispersion along ΓZ , and the value chosen is in qualitative accord with the LDA result. That CuO_2 plane parameters remain appropriate for the ladder confirms the predominantly local picture of the interactions between copper sites. Turning to the band splitting at the Γ and Z points, we find that the relatively large value $t_s = \frac{1}{2}t_r$ [Fig. 2(b)] gives the best qualitative reproduction of the bands crossing the chemical potential in the full LDA calculation by Mattheiss,¹⁵ but that the value $t_s = \frac{2}{5}t_r$ appears closer to the results of a ‘‘12-parameter fit’’ illustrated in the same reference. The difference of the Γ and Z splittings is given rather well by the starting choice of $t'_s = \frac{1}{5}t_s$.

It is clear from Fig. 2 that the primary feature of the dispersion remains that in the k_z direction, i.e., along the ladder. The Fermi surfaces for each band are determined almost exclusively by this part of the dispersion, in that they appear as sheets which are almost flat, perturbed little by the t_r and t_s terms, and have k_z as normal. At half-filling, the lowest band is an exception to this situation, because part of it is also filled close to the Z point. On doping with holes, this region is rapidly emptied (below 5%) so that all four Fermi surfaces are sheets parallel to the (k_x, k_y) plane. Only when the doping level reaches 20% does the chemical potential drop below the highest band in the $\Gamma XSY\Gamma$ plane, causing a pocket to open at the Γ point for this band.

In summary, we find that a simple model of a single orbital per copper atom provides a good fit to the band structure. While there is scope for some variation in the choice of intraladder parameters, with this level of agreement between the tight-binding results and those of LDA it is not worthwhile to optimize further. We choose to work with the above values of the intraladder hopping matrix elements, and with the interladder overlap $t_s = \frac{1}{2}t_r$, bearing in mind that this latter will be close to the upper limit of the narrow range of probable values. Estimating the superexchange interaction by $J' \propto 4t'^2/U$ leads us to conclude that the interaction between spins on neighboring ladders will have a magnitude $J' \approx 0.25J$, where J is the intraladder magnetic coupling of both rung and leg spins. Because J' is an appreciable fraction of J , it is clear that the spin interactions in $\text{LaCuO}_{2.5}$ will have significant three-dimensional character.

III. MEAN-FIELD ANALYSIS OF THE SPIN GROUND STATE

A mean-field analysis of the spin state for ladder systems was introduced by Gopalan *et al.*,¹⁹ and in this section we

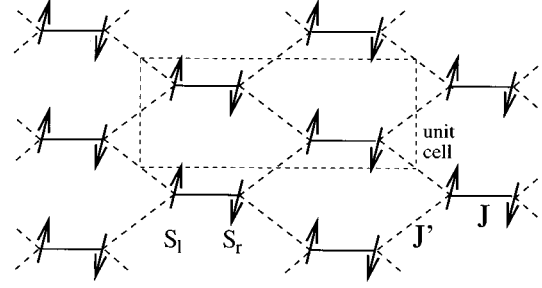


FIG. 3. Schematic representation of the periodic structure in the (x,y) plane of locally antiferromagnetically correlated spins, for calculation of the spinon dispersion. The magnetic interaction parameters shown are J on the ladder rungs and $J' \equiv \lambda J$ between spins on neighboring ladders.

follow closely the treatment of these authors. They employed a bond operator representation of $S = \frac{1}{2}$ quantum spins, used initially²⁰ to investigate dimerized spin phases in two-dimensional systems, exploiting the fact that the topology of the ladder favors dimerization, particularly when the spin interaction, J , on a rung exceeds that on a leg, λJ . The authors proceeded in the mean-field approximation to consider first the properties of an isolated ladder as a function of the interaction ratio λ , then of periodic arrays of ladders in two dimensions, and finally of an array of frustrated double ladders of the type found in the SrCu_2O_3 system.² This approach can be considered to be exact in the limit where $\lambda \rightarrow 0$ and the spins form dimers on every rung, while its accuracy will diminish on extrapolating through finite λ towards the desired isotropic point, $\lambda = 1$.

We begin by representing the system of spin ladders, each coupled by two identical bonds per spin to separate, neighboring ladders, in a geometrically simpler but topologically identical form, as shown in Fig. 3. Note that the spin configuration for local, antiferromagnetic interactions is unfrustrated, so a transition to an ordered antiferromagnet may be expected with increasing interladder coupling. The magnetic interactions are taken to be J for spins on the same rung, λJ for spins separated by a leg bond, and $\lambda' J$ for neighboring spins on different ladders, while no other couplings are considered. The Hamiltonian for the spins is

$$H = J \sum_j \mathbf{S}_{l,j} \cdot \mathbf{S}_{r,j} + \lambda J \sum_{j,m=l,r} \mathbf{S}_{m,j} \cdot \mathbf{S}_{m,j+\hat{z}} + \lambda' J \sum_j (\mathbf{S}_{r,j} \cdot \mathbf{S}_{l,j+\frac{1}{2}\hat{x}+\frac{1}{2}\hat{y}} + \mathbf{S}_{r,j} \cdot \mathbf{S}_{l,j+\frac{1}{2}\hat{x}-\frac{1}{2}\hat{y}}), \quad (6)$$

where j is a rung bond index and the labels l and r denote spins on the left and right sides of the ladder. Following Ref. 19, transformation to the bond-operator representation yields

$$H = H_0 + H_1 + H_2 + H_{\text{HO}}, \quad (7)$$

where

$$H_0 = J \sum_{j,\alpha} (-\frac{3}{4} s_j^\dagger s_j + \frac{1}{4} t_{j,\alpha}^\dagger t_{j,\alpha}) - \sum_{j,\alpha} \mu_j (s_j^\dagger s_j + t_{j,\alpha}^\dagger t_{j,\alpha} - 1), \quad (8)$$

$$H_1 = \frac{1}{2} \lambda J \sum_{j,\alpha} (t_{j,\alpha}^\dagger t_{j+\hat{z},\alpha}^\dagger s_{j+\hat{z}}^\dagger s_j + t_{j,\alpha}^\dagger t_{j+\hat{z},\alpha}^\dagger s_j s_{j+\hat{z}}^\dagger + \text{H.c.}) \quad (9)$$

and

$$H_2 = -\frac{1}{4} \lambda' J \sum_{j,\alpha} \sum_{\nu=\pm 1} (t_{j,\alpha}^\dagger t_{j+\frac{1}{2}\hat{x}+\nu\frac{1}{2}\hat{y},\alpha}^\dagger s_{j+\frac{1}{2}\hat{x}+\nu\frac{1}{2}\hat{y}}^\dagger s_j + t_{j,\alpha}^\dagger t_{j+\frac{1}{2}\hat{x}+\nu\frac{1}{2}\hat{y},\alpha}^\dagger s_j s_{j+\frac{1}{2}\hat{x}+\nu\frac{1}{2}\hat{y}}^\dagger + \text{H.c.}) \quad (10)$$

In these equations, s_j^\dagger is the creation operator for a spin singlet on bond j , the operators $t_{j,\alpha}^\dagger$ create the three possible triplet states on the same bond, and the Lagrange multiplier, μ_j , introduced to ensure the constraint

$$s_j^\dagger s_j + \sum_{\alpha} t_{j,\alpha}^\dagger t_{j,\alpha} = 1 \quad (11)$$

on each bond, which restricts the physical spin states to singlets or triplets, appears as an effective chemical potential. The part H_{HO} in (7) contains terms with three and four $t_{j,\alpha}$ operators, and will be neglected in our approximation; in Ref. 19 it was shown in addition that the effects of such higher-order terms are small.

Because the singlet on each bond has the lowest energy, we assume that the system condenses into this state, leading to a finite expectation value of the bosonic s_j operator, $\langle s_j \rangle = \bar{s}$. This is the average expectation value, or mean-field value of the operators s_j , and the site-dependent chemical potential μ_j is also replaced by a global average value μ . Working with the physical unit cell, which contains two rungs, we may transform the operators ($t_{j,\alpha}$) in H_0 , H_1 , and H_2 to those for two types of triplets, $t_{\mathbf{k}\alpha}^1$ and $t_{\mathbf{k}\alpha}^2$. The Hamiltonian in this approximation is²¹

$$H_m(\mu, \bar{s}) = N(-\frac{3}{4} J \bar{s}^{-2} - \mu \bar{s}^{-2} + \mu) + \sum_{\mathbf{k}\alpha} \left\{ \sum_{\nu=1,2} [\Lambda_{\mathbf{k}} t_{\mathbf{k}\alpha}^{\nu\dagger} t_{\mathbf{k}\alpha}^\nu + \Delta_{\mathbf{k}} (t_{\mathbf{k}\alpha}^{\nu\dagger} t_{-\mathbf{k}\alpha}^\nu + t_{\mathbf{k}\alpha}^\nu t_{-\mathbf{k}\alpha}^{\nu\dagger})] + [\Lambda'_{\mathbf{k}} t_{\mathbf{k}\alpha}^{1\dagger} t_{\mathbf{k}\alpha}^2 + \Delta'_k (t_{\mathbf{k}\alpha}^{1\dagger} t_{-\mathbf{k}\alpha}^2 + t_{\mathbf{k}\alpha}^1 t_{-\mathbf{k}\alpha}^2)] + [1 \leftrightarrow 2] \right\}, \quad (12)$$

in which

$$\Lambda_{\mathbf{k}} = \frac{1}{4} J - \mu + J \bar{s}^{-2} \lambda \cos k_z, \quad (13)$$

$$\Delta_{\mathbf{k}} = \frac{1}{2} J \bar{s}^{-2} \lambda \cos k_z, \quad (14)$$

$$\Lambda'_{\mathbf{k}} = 2 \Delta'_{\mathbf{k}} = -J' \bar{s}^{-2} \cos \frac{1}{2} k_x \cos \frac{1}{2} k_y, \quad (15)$$

and N denotes the total number of ladder rungs. The part of H_m (12) dependent on the triplet operators is diagonalized by the non-unitary, bosonic Bogoliubov transformation

$$\gamma_{\mathbf{k}\alpha}^\pm = \cosh \theta_{\mathbf{k}}^\pm (t_{\mathbf{k}\alpha}^1 \pm t_{\mathbf{k}\alpha}^2) + \sinh \theta_{\mathbf{k}}^\pm (\pm t_{-\mathbf{k}\alpha}^1 - t_{-\mathbf{k}\alpha}^2), \quad (16)$$

whose coefficients are given by

$$\cosh 2 \theta_{\mathbf{k}}^\pm = \frac{\Lambda_{\mathbf{k}} + \Lambda'_{\mathbf{k}}}{\omega_{\mathbf{k}}^\pm}, \quad \sinh 2 \theta_{\mathbf{k}}^\pm = \frac{2(\Delta_{\mathbf{k}} \pm \Delta'_{\mathbf{k}})}{\omega_{\mathbf{k}}^\pm}. \quad (17)$$

where in turn

$$\omega_{\mathbf{k}}' = \sqrt{(\Lambda_{\mathbf{k}} \pm \Lambda'_{\mathbf{k}})^2 - 4(\Delta_{\mathbf{k}} \pm \Delta'_{\mathbf{k}})^2} \quad (18)$$

yield the dispersion relations of the two magnon branches. The Hamiltonian now takes the form

$$H_m(\mu, \bar{s}) = N(-\frac{3}{4} J \bar{s}^{-2} - \mu \bar{s}^{-2} + \mu) - \frac{3}{2} N(\frac{1}{4} J - \mu) + \sum_{\mathbf{k}\alpha} \sum_{\nu=\pm} \omega_{\mathbf{k}}^\nu (\gamma_{\mathbf{k}\alpha}^{\nu\dagger} \gamma_{\mathbf{k}\alpha}^\nu + \frac{1}{2}), \quad (19)$$

which contains the mean-field part and the zero-point quantum corrections from the triplet magnon excitations. The mean-field equations to be solved self-consistently for μ and \bar{s} are given by

$$\left\langle \frac{\partial H_m}{\partial \mu} \right\rangle = 0 = \bar{s}^{-2} - \frac{5}{2} + 3 \sum_{\mathbf{k}\nu=\pm} \frac{\Lambda_{\mathbf{k}} + \nu \Delta'_{\mathbf{k}}}{4 \omega_{\mathbf{k}}^\nu} n_m(\omega_{\mathbf{k}}^\nu) \quad (20)$$

and

$$\left\langle \frac{\partial H_m}{\partial \bar{s}} \right\rangle = 0 = \frac{3}{2} + 2 \frac{\mu}{J} - 3 \sum_{\mathbf{k}\nu=\pm} \frac{\Lambda_{\mathbf{k}} - 2 \Delta_{\mathbf{k}}}{2 \omega_{\mathbf{k}}^\nu} a_{\mathbf{k}}^\nu n_m(\omega_{\mathbf{k}}^\nu), \quad (21)$$

where

$$a_{\mathbf{k}}^\pm = \lambda \cos k_z \pm \lambda' \cos \frac{1}{2} k_x \cos \frac{1}{2} k_y \quad (22)$$

contain the dispersive parts of $\omega_{\mathbf{k}}^\pm$. $n_m(\omega_{\mathbf{k}}^\pm)$ denotes the magnon thermal occupation function, and will be discussed in more detail in a future publication. The factor of 3 preceding the \mathbf{k} summations in both equations is the result of the sum over α for the three triplet magnon states.²¹ This factor was omitted in Ref. 19, and we comment below on the effect of the correction on the results presented there.

The mean-field equations are solved at zero temperature, where the thermal factor becomes unity, and by taking the continuum limit in which the \mathbf{k} sum becomes an integral over three-dimensional reciprocal space. As in Ref. 19 we reduce the two equations to a single one for the variable

$$d = \frac{2J \bar{s}^{-2}}{\frac{1}{4} J - \mu}, \quad (23)$$

which has the form

$$d = 5 - 3 \sum_{\nu=\pm} \int \frac{d^3 k}{(2\pi)^3} \frac{1}{\sqrt{1 + d a_{\mathbf{k}}^\nu}}. \quad (24)$$

As a characteristic parameter of the spin-liquid ground state, we will be most interested in the value of the spin gap, the minimum excitation energy of the triplet magnon excitations, which is given by

$$\Delta = (\frac{1}{4} J - \mu) \sqrt{1 - d(\lambda + \lambda')}, \quad (25)$$

with d determined by the mean-field equation (24). From Eq. (16) we see that the excitation spectrum has a minimum at the wave vector $\mathbf{k}_M = (0, 0, \pi)$ in the reciprocal lattice of the bipartite structure shown in Fig. 3. The value of λ' where Δ is driven to zero will give the transition from the spin

liquid state, where the spin orientation fluctuates with a time-averaged value of zero and with short-range correlations primarily at \mathbf{k}_M , to a magnetically ordered state characterized by \mathbf{k}_M . This wave vector corresponds to uniform polarization of the spin singlets on ladder rungs in the (x,y) plane, with spins oppositely directed between neighboring planes in the z direction, i.e., a simple antiferromagnetically aligned spin pattern.

In the limit of no interladder coupling we obtain the spin gap $\Delta_0 = 0.501J$ of the isolated, isotropic ($\lambda = 1$) two-leg ladder. This is only a mean-field result, but is in very good agreement with the result $\Delta_0 = 0.504J$ of numerical studies⁹ by the density matrix renormalization group technique. In fact this agreement is largely serendipitous, and deteriorates on taking into account the higher-order terms;²² in the mean-field approximation, the spin gap of the isolated ladder diverges logarithmically in the limit of large λ ,¹⁹ and the effects of this increase are already manifest at $\lambda = 1$, causing the mean-field result, which initially underestimates the spin gap, to recover towards the exact value determined numerically. In this treatment we have not had to invoke a self-energy correction term: in Ref. 19, the authors investigated the curious qualitative behavior of the solution to their (erroneous) mean-field equation by expanding in small λ about the limit of strong rung coupling where the dimer treatment is accurate. In the corrected mean-field theory, one obtains

$$\Delta = J(1 - \lambda + \frac{1}{4}\lambda^2 + \frac{3}{8}\lambda^3 + O(\lambda^4)), \quad (26)$$

which corresponds reasonably well to the result

$$\Delta = J(1 - \lambda + \frac{1}{2}\lambda^2 + \frac{1}{4}\lambda^3 + O(\lambda^4)) \quad (27)$$

of a detailed strong-coupling analysis including excitation modes.²³ Previously, the coefficient of the quadratic term had been found to be negative, and so a self-energy term $\beta\lambda^2$ was introduced to correct for short-range interaction effects which appeared to have been missing at the mean-field level; the chosen value $\beta = 0.7$ brought the results into good agreement with previous numerical ones, and with the above approximate treatments.

The spin gap obtained from the solution of (24) for the three-dimensionally coupled ladder system is shown in Fig. 4(a) as a function of the interladder coupling λ' , for fixed $\lambda = 1$. We see immediately that the spin gap decreases monotonically, with the transition point at $\lambda' = 0.121$. Comparison with the result of Sec. II indicates that the $\text{LaCuO}_{2.5}$ system should lie within the ordered antiferromagnetic regime, but that it is indeed located in the vicinity of the quantum critical point marking the phase transition from spin liquid to magnetic order.

It is also instructive to compare the appearance of the spin gap with that in a two-dimensional, unfrustrated periodic array of coupled ladders.¹⁹ In this case the dispersive factor in the excitation spectrum will be

$$a_{\mathbf{k}} = \lambda \cos k_z - \frac{1}{2}\lambda' \cos k_x, \quad (28)$$

where k_x is a wave vector parallel to a ladder rung. Again $\mathbf{k}_M = (0, \pi)$ corresponds to a simple antiferromagnetic spin alignment in the ordered phase, and the factor of $\frac{1}{2}$ appears because there is only one bond between ladders per spin in such a system. The spin gap for the two-dimensional array is

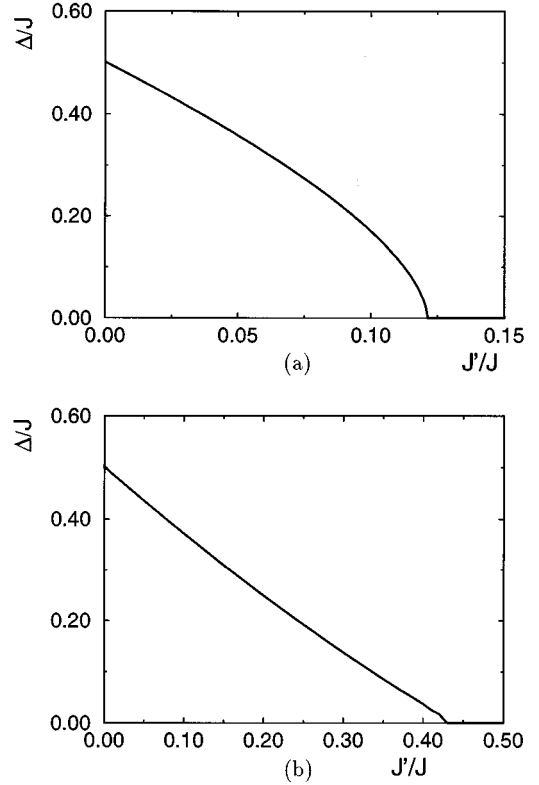


FIG. 4. (a) Spin gap Δ as a function of the ratio between interladder and intraladder magnetic couplings J'/J , calculated for a three-dimensional system at $T=0$, in the mean-field approximation from the starting point of dimerized ladder rungs. Here the intraladder rung and leg interactions are the same ($\lambda = 1$), and the value of the spin gap at $J'=0$ is that of the noninteracting, two-leg ladder ($\Delta_0 = 0.501J$) in the same approximation. (b) Spin gap for a two-dimensional array of ladders.

shown as a function of λ' in Fig. 4(b), where again $\lambda = 1$ and the gap at $\lambda' = 0$ is that of the isolated, isotropic ladder. The critical value of the interladder coupling, $\lambda'_c = 0.43$, is seen to be significantly greater than twice that in the three-dimensional case above, as might be expected for the simple reason that there are half as many interladder interactions, which may be taken as an indication that the spin liquid state is more robust in lower dimensions. The almost linear decrease, in contrast to the downward curvature of the function in Fig. 4(a), illustrates the most significant effect of dimensionality, and agrees well with the qualitative result of Ref. 19.

We may conclude that to within the accuracy of the mean-field approach for an isotropic ladder system, the above analysis provides good evidence that $\text{LaCuO}_{2.5}$ lies on the magnetically ordered side of the quantum critical regime of the transition between spin liquid and antiferromagnet.

IV. HARTREE-FOCK APPROXIMATION TO THE HUBBARD MODEL

We have seen in the previous sections that the interladder interactions in $\text{LaCuO}_{2.5}$ are quite strong, and possibly sufficiently strong to change the magnetic structure from a spin liquid to a three-dimensionally ordered antiferromagnet. To examine further the character of the electronic structure, we

introduce an on-site Coulomb interaction, U , to the tight-binding band structure of Sec. II, and perform a Hartree-Fock calculation of an ordered antiferromagnetic state. In a strictly one-dimensional system, the critical value of U necessary to stabilize an insulating antiferromagnet vanishes at half-filling, whereas in a general, three-dimensional electronic structure it is of the order of the bandwidth.

Introduction of the on-site Coulomb interaction leads to a Hubbard Hamiltonian

$$H_{\text{HM}} = - \sum_{ij\sigma} t_{ij} c_{i\sigma}^\dagger c_{j\sigma} + U \sum_i c_{i\uparrow}^\dagger c_{i\uparrow} c_{i\downarrow}^\dagger c_{i\downarrow}. \quad (29)$$

Examining the stability of an antiferromagnetic state with wave vector \mathbf{k}_M , we note first that there will be no increase of the unit cell in the (x,y) plane, since there are already two atoms for each spin direction, but that it doubles along \hat{z} when the spins order along the ladder legs. In the notation of A and B sublattices for the bipartite system, sites $m=1,3$ of the original unit cell [Fig. 1(c)] in every second plane, and $m=2,4$ in the alternating planes, will belong to the A sublattice, while the remaining sites will belong to B . Introducing the parameter $\delta n_A = n_\uparrow - n_\downarrow$ as the difference between average site occupation by particles of each spin orientation on a site of the A sublattice, we require $\delta n_A = -\delta n_B = \delta n$ for all sites. We proceed by solving the problem in the Hartree-Fock approximation, with the value of U where δn becomes finite marking the antiferromagnetic transition.

Following the treatment of Sec. II, the Hamiltonian may be written as in Eq. (2), with now $\mathbf{c}_{\mathbf{k}\sigma}^\dagger = (c_{\mathbf{k}\sigma}^{1a\dagger}, c_{\mathbf{k}\sigma}^{1b\dagger}, \dots)$, where the superscripts a and b denote atoms in the two (x,y) planes of the doubled unit cell, and

$$\mathbf{H}_{\mathbf{k}} = - \begin{pmatrix} \mathbf{M}_+ & \mathbf{S}(k_z) & \mathbf{0} & \bar{\mathbf{R}}^*(k_z) \\ \mathbf{S}^*(-k_z) & \mathbf{M}_- & \mathbf{R}(k_z) & \mathbf{0} \\ \mathbf{0} & \mathbf{R}^*(-k_z) & \mathbf{M}_+ & \mathbf{S}(k_z) \\ \bar{\mathbf{R}}(-k_z) & \mathbf{0} & \mathbf{S}^*(-k_z) & \mathbf{M}_- \end{pmatrix}, \quad (30)$$

in which the 2×2 matrices

$$\mathbf{M}_\pm = \begin{pmatrix} 2t'_z \cos k_z \pm \frac{1}{2} U \delta n & t_z e^{i1/2k_z} \\ t_z e^{-i1/2k_z} & 2t'_z \cos k_z \mp \frac{1}{2} U \delta n \end{pmatrix}, \quad (31)$$

$$\mathbf{R}(k_z) = \begin{pmatrix} t_r e^{i\mathbf{k} \cdot \mathbf{r}} & t'_r e^{i\mathbf{k} \cdot \mathbf{r} + i\frac{1}{2}k_z} \\ t'_r e^{i\mathbf{k} \cdot \mathbf{r} - i\frac{1}{2}k_z} & t_r e^{i\mathbf{k} \cdot \mathbf{r}} \end{pmatrix}, \quad (32)$$

$\bar{\mathbf{R}}(k_z)$ (defined identically using) and

$$\mathbf{S}(k_z) = \begin{pmatrix} t_s \cos \frac{1}{2} k_x e^{ik_y s_y} & t'_s \cos \frac{1}{2} k_x e^{ik_y s_y + i1/2k_z} \\ t'_s \cos \frac{1}{2} k_x e^{ik_y s_y - i1/2k_z} & t_s \cos \frac{1}{2} k_x e^{ik_y s_y} \end{pmatrix} \quad (33)$$

are the generalizations of the previous expressions to the new unit cell, and the new c -axis dimension is set to unity. This matrix cannot be block diagonalized, but the structure of the solution for the eigenmodes and eigenvectors is evident from Sec. II. Schematically, if the (k_x, k_y) dispersion contained in

the square root in Eq. (5) is denoted by $\bar{\epsilon}_{\mathbf{k}}^2$ the eight band dispersions will have the form

$$E_{\mathbf{k}}^i = \pm [\bar{\epsilon}_{\mathbf{k}}^2 + 4t_z^2 \cos^2 \frac{1}{2} k_z \pm \frac{1}{4} U^2 \delta n^2]^{1/2} - 2t'_z \cos 2k_z, \quad (34)$$

where i labels the bands. The $U \delta n$ term splits the former four bands into two sets, which as U becomes large will not overlap, ensuring that the half-filled system becomes insulating. The corresponding eigenvectors are the states

$$\psi_{\mathbf{k}}^i = \sum_{j=1}^8 C_j^i \phi_{\mathbf{k}}^j, \quad (35)$$

where the index j runs over the eight atomic sites, and $\phi_{\mathbf{k}}^j$ is the Bloch state created by the operator $c_{\mathbf{k}}^{j\dagger}$. The Hartree-Fock equations for the system, which will determine δn and the chemical potential μ at fixed U when solved self-consistently, are the equations for the total and site occupancies

$$1 - \delta = \frac{1}{4} \sum_{i=1}^8 \int \frac{d^3 k}{(2\pi)^3} \frac{1}{e^{\beta \xi_{\mathbf{k}}^i} + 1} \quad (36)$$

and

$$\frac{1}{2} (1 - \delta) (1 + \delta n) = \sum_{i=1}^8 \int \frac{d^3 k}{(2\pi)^3} \frac{|C_j^i|^2}{e^{\beta \xi_{\mathbf{k}}^i} + 1}. \quad (37)$$

These equations have been generalized to arbitrary band filling, which is expressed in terms of the deviation δ from half-filling, which in turn is normalized to be 1. The chemical potential is contained in $\xi_{\mathbf{k}}^i = E_{\mathbf{k}}^i - \mu$, and the second expression is valid for the coefficients of any chosen Bloch function j .

The operation of diagonalizing the Hamiltonian matrix (29) can be performed numerically at sufficient speed that it is still possible to solve the Hartree-Fock equations, which involve three-dimensional \mathbf{k} integration, on a workstation within a reasonable amount of time. In Fig. 5(a) are shown the energy bands for the incipient antiferromagnetic system for half-filling ($\delta=0$) and $U=t$. The splitting of the bands into upper and lower branches as a result of U is clearly evident, as is the characteristic $\Gamma XSY\Gamma$ and $ZURTZ$ structure of the purely kinetic Hamiltonian in both sets of bands, at positive and negative energies, as a result of the folding back of bands due to the change in meaning of the coordinate k_z , which now spans a Brillouin zone half the former size. At this value of U , the half-filled system would appear to be close to the transition from metallic to insulating behavior, which one expects near the point where there is no longer any overlap between upper and lower band energies in any region of reciprocal space. At smaller values of U , the two sets of bands are characteristic of the doubled Brillouin zone, and have a semimetallic overlap, while as U is raised to large values, the energy gap increases, and the bands become progressively more flat.

In other cuprate compounds, a Hubbard model has been found²⁴ to give an accurate description of the low-energy behavior with a ratio U/W of order unity, where W is the bandwidth. Here the total bandwidth of the uppermost va-

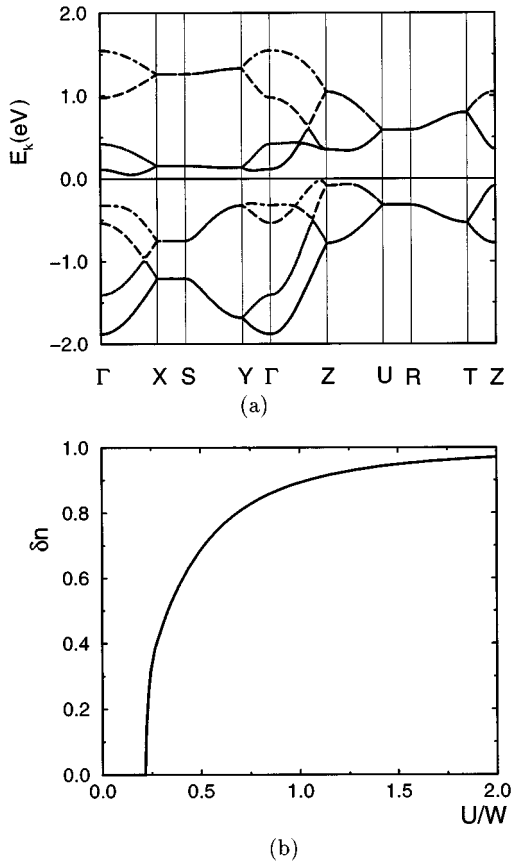


FIG. 5. (a) Band structure computed in the Hartree-Fock approximation for the parameters of the tight-binding fit of Sec. II, with the inclusion of an on-site repulsion parameter U . The bands are shown for $U=t=0.4$ eV, where the half-filled system is close to the metal-insulator transition. (b) Antiferromagnetic order as a function of U . The degree of ordering is parameterized by $\delta n = n_{\uparrow} - n_{\downarrow}$, the difference between the average occupation of each site in the structure by particles with spins oriented upwards and downwards. The doping is $\delta=0$, i.e., the system is half-filled, and the temperature is taken to be low.

lence bands is approximately the same as in the cuprates with CuO_2 planes, $W \approx 3$ eV. Since the local environment of the Cu^{2+} ions is similar, the on-site Coulomb repulsion should also be the same, $U \approx 4$ eV. These parameter values place $\text{LaCuO}_{2.5}$ well within the Mott insulating region. We note that the actual magnetic structure cannot be determined in the Hartree-Fock approximation, as the quantum corrections which act to stabilize the spin liquid phase are not included.

The form of the Hartree-Fock solutions for smaller values of U are sensitive to the effective dimensionality of the electronic structure. In general, values of $U \sim W$ are required to obtain a Mott insulator at half-filling, but the perfect-nesting property of a one-dimensional band gives an insulating state for arbitrarily small values of U . In Fig. 5(b), the average antiferromagnetic order (parameterized by δn) in the half-filled system is shown as a function of the on-site repulsion U , which is measured in terms of the bandwidth $W \equiv 3$ eV. In $\text{LaCuO}_{2.5}$ we find that the critical value U_c for the antiferromagnetic transition is rather small, $U_c \approx 0.2W$, which indicates substantial one-dimensional nature. The interladder

hopping matrix elements, although quite strong, are not sufficient to destroy the nesting character completely, which would make the electronic structure effectively three dimensional.

This quasi-one-dimensional behavior of the bands may also be reflected in the sensitivity of the system to random potential fluctuations. It is well known that the onset of localization is strongly dependent on dimensionality. Clearly, in ladder compounds there is an inherent conflict between the need to change the valence of the counterions in order to induce hole carriers, and the need to avoid strong, random potential fluctuations. Thus it appears that in $\text{La}_{1-x}\text{Sr}_x\text{CuO}_{2.5}$ the random potential fluctuations act to cause localization for $x \leq 0.15$, in spite of the substantial interladder overlap, suggesting that a more gentle hole-doping technique will be required to retain itinerant character at small doping concentrations. This could perhaps be achieved in structures where the counterions are further from the ladders than in the present case of $\text{LaCuO}_{2.5}$.

V. CONCLUSION

We have investigated the basic electronic and magnetic properties of the three-dimensionally coupled two-leg ladder compound $\text{LaCuO}_{2.5}$, a material which is of significant experimental and theoretical interest as it is the first ladder compound to be discovered in which the Cu_2O_3 ladders may be doped with holes. We present a tight-binding fit in which the bands are derived from a single ($d_{x^2-y^2}$) orbital close to the Fermi energy on each copper atom. The results of LDA studies are well reproduced by reasonable values of the most significant transfer integrals: those within each ladder are found to be similar to the CuO_2 planar system, emphasizing the short-range nature of the dominant physical processes, while the interladder hopping term $t' \approx \frac{1}{2}t$ is found to be quite large. As a consequence, the interladder magnetic coupling J' is also relatively large, and the compound may be expected to exhibit some three-dimensional characteristics.

The effective spin interactions in this structure are those of unfrustrated antiferromagnetism, and a mean-field treatment of the magnetic state from the basis of dimerized singlets on the rungs of decoupled ladders gives a spin-liquid phase whose spin gap decreases with increasing interladder coupling. The spin gap is found to vanish, signaling a transition to an ordered phase, at an interladder coupling ratio J'/J somewhat smaller than that deduced for $\text{LaCuO}_{2.5}$, indicating that the system is located in the antiferromagnetically ordered state, albeit not far from the quantum critical point of the ordering transition. We may take the very small value of the intrinsic susceptibility measured at low temperatures¹² as evidence that proximity to the critical point, and the possibility this allows of significant critical fluctuations, plays an important role in determining the physics of the system.

Further insight into the electronic properties is provided by the introduction of an on-site repulsion term, U , to the band scheme: within the Hartree-Fock approximation we find that in the half-filled system the transition to an antiferromagnetic insulator occurs for values of U quite small compared to the bandwidth. This is a reflection of the fact that the predominant feature of the bands remains the dispersion

in the ladder direction, and this one-dimensionality, also apparent in the Fermi surfaces of the partially-filled bands, makes the system inherently susceptible to potential fluctuations. That U_c is finite illustrates an absence of perfect nesting conditions in the band structure, and the instability occurs at the antiferromagnetic wave vector.

Our results represent the first theoretical consideration of the $\text{LaCuO}_{2.5}$ system. While by the nature of the approximate techniques used they are somewhat inexact, we believe that they are important in establishing the parameter space for the magnetic state, and in focussing the direction of further research. The properties of such “nearly critical” magnetic systems have been studied for the two-dimensional, planar case by detailed analytical²⁵ and numerical²⁶ techniques. We propose the application of similar methods for the case of ladder systems with variable interladder coupling in two additional dimensions, to investigate the nature of the critical point, and the surrounding “quantum critical” regime, in the same formalism, with particular emphasis on the appearance of physical quantities accessible in experiment. Such studies may prove valuable in establishing the framework within which to interpret the data from experiment, and hopefully

will serve to reconcile the apparent contradiction in current results.

The observation that the spin liquid is not the appropriate description of the magnetic ground state is itself important, particularly with regard to the current interpretation of the susceptibility data.¹² While it may be possible to deduce the form of the susceptibility suitable for the critical regime from a mean-field picture, we await the results of numerical studies of the same system in order to make a more detailed comparison with the data. A further direction not strongly emphasized in this communication is the nature of the doped system: the methods used here become less accurate at finite doping, and so were not studied in great detail in this regime, but may nonetheless be used to obtain additional insight into the evolution of spin properties on moving towards the metallic state.

ACKNOWLEDGMENTS

We are grateful to Y. Kitaoka, M. Sigrist, M. Takano, M. Troyer, and especially Z. Hiroi and M. Zhitomirsky for helpful discussions, and to the Swiss National Fund for financial support.

¹E. Dagotto and T. M. Rice, *Science* **271**, 618 (1996).

²Z. Hiroi, M. Azuma, M. Takano, and Y. Bando, *J. Solid State Chem.* **95**, 230 (1991).

³T. M. Rice, S. Gopalan, and M. Sigrist, *Europhys. Lett.* **23**, 445 (1993).

⁴M. Azuma, Z. Hiroi, M. Takano, K. Ishida, and Y. Kitaoka, *Phys. Rev. Lett.* **73**, 3463 (1994).

⁵K. Ishida, Y. Kitaoka, K. Asayama, M. Azuma, Z. Hiroi, and M. Takano, *J. Phys. Soc. Jpn.* **63**, 3222 (1994).

⁶E. Dagotto, J. Riera, and D. J. Scalapino, *Phys. Rev. B* **45**, 5744 (1992).

⁷R. Hirsch, *Diplomarbeit*, Universität Köln, 1988.

⁸T. Barnes, E. Dagotto, J. Riera, and E. Swanson, *Phys. Rev. B* **47**, 3196 (1993).

⁹S. White, R. Noack, and D. J. Scalapino, *Phys. Rev. Lett.* **73**, 886 (1994).

¹⁰B. Frischmuth, B. Ammon, and M. Troyer (unpublished).

¹¹G. Sierra (unpublished).

¹²Z. Hiroi and M. Takano, *Nature* **377**, 41 (1995).

¹³M. Troyer, H. Tsunetsugu, and D. Würtz, *Phys. Rev. B* **50**, 13 515 (1994).

¹⁴S. Matsumoto, Y. Kitaoka, K. Ishida, K. Asayama, Z. Hiroi, N.

Kobayashi, and M. Takano, *Phys. Rev. B* **53**, 11 942 (1996).

¹⁵L. F. Mattheiss, *Solid State Commun.* **97**, 751 (1996).

¹⁶P. W. Anderson, in *Magnetism I*, edited by G. T. Rado and H. Suhl (Academic Press, New York, 1963).

¹⁷T. Tanamoto, H. Kohno, and H. Fukuyama, *J. Phys. Soc. Jpn.* **62**, 717 (1993).

¹⁸B. Normand, H. Kohno, and H. Fukuyama, *J. Phys. Soc. Jpn.* **64**, 3903 (1995).

¹⁹S. Gopalan, T. M. Rice, and M. Sigrist, *Phys. Rev. B* **49**, 8901 (1994).

²⁰S. Sachdev and R. Bhatt, *Phys. Rev. B* **41**, 9323 (1990).

²¹We are indebted to M. E. Zhitomirsky for pointing out to us an error in the original version of the following calculation.

²²M. E. Zhitomirsky, O. A. Starykh, and K. Ueda (private communication).

²³M. Reigrotzki, H. Tsunetsugu, and T. M. Rice, *J. Phys. Condens. Matter* **6**, 9325 (1994).

²⁴M. Hybertsen, E. B. Stechel, M. Schlüter, and D. R. Jennison, *Phys. Rev. B* **41**, 11 068 (1990).

²⁵A. V. Chubukov, S. Sachdev, and J. Ye, *Phys. Rev. B* **49**, 11 919 (1994).

²⁶M. Troyer (private communication).